Aromatic compounds and organic acids identified from *Ganoderma formosanum* exhibit synergistic anti-melanogenic effects

Chen-Che Hsieh [a,1], Chih-Yao Hou [b,1], Hsiao-Yun Lei [a], Darin Khumsupan [c], Huey-Jine Chai [d], Pek-Kui Lim [e], Cheng-Chih Hsu [f], Sz-Jie Wu [g], Kai-Wen Cheng [f], Yi-Chen Chen [h,i,**], Kuan-Chen Cheng [a,c,j,k,*]

[a] Institute of Food Science Technology, National Taiwan University, No. 1, Sec. 4, Roosevelt Rd., Taipei, Taiwan, R.O.C.
[b] Department of Seafood Science, College of Hydrosphere, National Kaohsiung University of Science and Technology, Kaohsiung 81157, Taiwan, R.O.C.
[c] Institute of Biotechnology, National Taiwan University, No. 1, Sec. 4, Roosevelt Rd., Taipei, Taiwan, R.O.C.
[d] Seafood Technology Division, Fisheries Research Institute, Ministry of Agriculture, Keelung 20246, Taiwan, R.O.C.
[e] School of Food Studies and Gastronomy, Taylor's University, Subang Jaya, Selangor 47500, Malaysia
[f] Department of Chemistry, National Taiwan University, No. 1, Sec. 4, Roosevelt Rd., Taipei 10617, Taiwan, R.O.C.
[g] Department of Horticulture and Landscape Architecture, National Taiwan University, Taipei, Taiwan, R.O.C.
[h] Department of Animal Science and Technology, National Taiwan University, Taipei 106, Taiwan, R.O.C.
[i] The Master Program in Global Agriculture Technology and Genomic Sciences, International College, National Taiwan University, Taipei 106, Taiwan, R.O.C.
[j] Department of Optometry, Asia University, 500, Lioufeng Rd., Wufeng, Taichung, Taiwan, R.O.C.
[k] Department of Medical Research, China Medical University Hospital, China Medical University, 91, Hsueh-Shih Road, Taichung, Taiwan, R.O.C.

Abstract

This study reveals the anti-tyrosinase activity of *Ganoderma formosanum* extracts, pinpointing compounds including gluconic acid, mesalamine, L-pyroglutamic acid, esculetin, 5-hydroxyindole, and salicylic acid, as effective melanin production inhibitors in melanoma cells and zebrafish embryos. Furthermore, multiple molecular docking simulations provided insights into interactions between the identified compounds and tyrosinase, increasing binding affinity up to −16.36 kcal/mol. The enhanced binding of identified compounds to tyrosinase facilitated synergistic inhibitory effects on melanin production. This study highlights the potential of GFE-EA as a source of natural tyrosinase inhibitors and contributes to understanding the role of active compounds extracted from *G. formosanum*.

Keywords: Anti-melanogenesis, Depigmentation, *Ganoderma formosanum*, Synergistic effects, Tyrosinase inhibition

1. Introduction

Melanin, synthesized as a byproduct of melanocytes, acts as a natural protector against harmful ultraviolet (UV) radiation [1]. Tyrosinase is a crucial enzyme in melanogenesis and the overproduction of melanin can lead to cosmetic issues such as melasma and hyperpigmentation. Traditional medicines like koji acid (KA), corticosteroids, and hydroquinone are commonly used to treat these conditions, but they can cause side effects, such as irritation and toxicity [2].

Ganoderma formosanum (*G. formasanum*), an endemic species to Taiwan and a variant of *Ganoderma. sinense*, was discovered on the trunk of a Chinese sweet gum in the mountainous region of Taoyuan three decades ago [3]. This fungus has been recognized for its ability to scavenge free radicals,

Received 26 March 2024; accepted 20 May 2024.
Available online 15 December 2024

* Corresponding author at: Institute of Food Science Technology, National Taiwan University, No. 1, Sec. 4, Roosevelt Rd., Taipei, Taiwan.
** Corresponding author at: Department of Animal Science and Technology, National Taiwan University, Taipei 106, Taiwan.
E-mail addresses: ycpchen@ntu.edu.tw (Y.-C. Chen), kccheng@ntu.edu.tw (K.-C. Cheng).
[1] Dr. Chen-Che Hsieh and Dr. Chih-Yao Hou are co-first authors who contributed equally to the manuscript writing and experimental execution.

https://doi.org/10.38212/2224-6614.3509

inhibit the proliferation of human prostate cancer cells, exert immunoregulatory effects, induce hepatoprotective bioactivity, and enhance melatonin production [4–7]. It has been reported that tyrosinase can be inhibited by *G. formosanum*, However, past studies had only confirmed that extracts of *G. formosanum* possess whitening effects, and the specific active compounds within the extracts remained to be clarified and discovered [6,8]. As a result, the extracts from *G. formosanum*, widely recognized for their anti-melanogenic properties, have been incorporated into natural tyrosinase inhibitors [9].

Meanwhile, molecular docking is a computational technique that simulates and analyzes the interactions between small and larger molecules, such as proteins and ligands. For instance, the hexapeptide from *G. lucidum* found structure-related tyrosinase–inhibitory activity, which was explained by molecular docking [10]. Three polyphenols from food had synergistic groups that increased the spontaneity of the binding process on anti-tyrosinase [11]. Understanding the interactions between them is critical in molecular identification and virtual drug screening, which have the benefit of anti-melanogenesis agents derived from edible natural food [12].

This study aimed to elucidate the anti-melanogenesis properties of the ethyl acetate fraction of the ethanol extract from *G. formosanum* (GFE-EA). The obtained fractions of the extract were validated for their anti-melanogenesis activities through a combination of *in vitro* tyrosinase enzymatic assays, thin layer chromatography (TLC), melanoma cells, and a zebrafish model. Additionally, the anti-melanogenesis-inducing compounds in GFE-EA were identified using ultra-high-performance liquid chromatography-tandem mass spectrometry (UHPLC-MS/MS). Furthermore, molecular docking simulations were employed to investigate the potential synergistic interactions between the identified compounds and tyrosinase, aiming to demonstrate their potential for enhanced tyrosinase inhibition.

2. Material and methods

2.1. Materials

G. formosanum was purchased from American Type Culture Collection (Rockville, MD., U.S.A.), and B16-F10 cell line was obtained from Bioresource Collection and Research Center (BCRC) (Hsinchu, Taiwan). Zebrafish was obtained from NTU Tech Comm. (Taipei, Taiwan). Medium ingredients such as peptone, yeast extract, potato dextrose broth, and agar were purchased from BioShop Canada Inc. (Ontario, Canada). Ethylenediaminetetraacetic acid solution (EDTA), trypsin, and antibiotics (penicillin/streptomycin) were purchased from GE Healthcare Life Science (Logan, Utah, U.S.A). Cell culture media (Dulbecco's Modified Eagle Medium, or DMEM, supplemented with high glucose, phenol red, and L-glutamine) and fetal bovine serum were obtained from GE Healthcare Life Science. Radio-Immunoprecipitation Assay (RIPA) Buffer (10X) was obtained from Cell Signaling Technology (Beverly, MA, U.S.A). Cell Counting Kit-8 (CCK-8) was purchased from Cyrus Bioscience (Neihu, Taiwan). Sephadex® LH-20 resin used for column chromatography was obtained from GE Healthcare Life Science (Uppsala, Sweden). All chemicals used in this study were of analytical grade and purchased from Merck (Burlington, MA, U.S.A).

Abbreviations

ESI	electrospray ionization
HPLC-DAD	high-performance liquid chromatography with photodiode-array detection
LC-MS/MS	liquid chromatography-tandem mass spectrometry
PBS	phosphate-buffered saline
TLC	thin-layer chromatography

2.2. Submerged cultivation of G. formosanum

The cultivation and activation of *G. formosanum* were performed on a plate with potato dextrose agar. Six mycelium blocks (with an approximate total surface area of 923.64 mm^2) were obtained from the outermost layer of the cultivated fungi by using a puncher with a diameter of 14 mm. The blocks were then cultivated in a 250-mL Erlenmeyer flask containing 100 mL of the growth medium for seven days. The cultivation temperature was maintained at 25 °C and the agitation speed was set at 150 rpm. Subsequently, the cultivated inoculum was loaded into a homogenizer to create a mycelium mixture. Next, 250 mL of the homogenized mixture was loaded into a 3-L fermenter containing 2250 mL of the submerged cultivation medium. The fermenter was maintained at 25 °C, agitated at 130 rpm, and subjected to an aeration rate of 1 vvm. Finally, mycelia were collected after seven days in dark environment of cultivation [6,13].

2.3. Purification of depigmenting components in G. formosanum

The methods previously reported by Ballinger et al. (2011) and Lehbili et al. (2018) were referenced

and adapted with modifications in this study [14,15]. Column chromatography (Sephadex® LH-20; eluted with methanol) was performed to fractionate different compounds in GFE-EA. The elution volume was five times that of the column volume, in which 500 mL of methanol was eluted at a rate of 1 mL/min. A total of 88 fractions (F1–F88) were collected at volume intervals of 6 mL from this LH-20 column chromatography [16].

2.4. Anti-melanogenesis effects of G. formosanum analyzed by a thin-layer chromatography (TLC) method

The analysis of the collected fractions was conducted following a method previously reported by Hsu et al. (2018) with modifications. A 20 mM phosphate buffer was used to prepare tyrosinase (1000 units/mL) and 10 mM levodopa solutions. Next, 2 μL of a collected fraction sample, kojic acid (KA, positive control), and methanol (negative control) were loaded onto a TLC plate and settled for 5 min. The step was repeated three times for each fraction samples, positive control, and negative control, resulting in three spots on the TLC plate. Subsequently, each sample spot on the TLC plate was applied with 1 μL of tyrosinase solution (1000 unit/mL) and left to settle for 5 min. Next, 2 μL of 10 mM levodopa solution was applied to each spot and the plate was left to stand in the darkness for 10 min to allow the reactions to occur. After all reactions were completed, the plate was immediately scanned and analyzed using ImageJ (National Institutes of Health, U.S.A.) [17,18].

2.5. Non-target analysis of depigmenting components in G. formosanum

This study used a high-performance liquid chromatography-diode array detector (HPLC-DAD) system (Agilent 1260 Infinity) with a detection wavelength range of 190–600 nm. The predominant absorption wavelength was identified among 254, 300, and 365 nm [6,19]. For non-target analysis of the fermented products, a Vanquish UHPLC-DAD (Thermo Scientific™) system coupled with an Orbitrap Elite™ Hybrid Ion Trap-Orbitrap Mass Spectrometer was employed. The flow rate was maintained at 0.5 mL/min, and the column temperature was held at 25 °C. A gradient elution approach was adopted with two mobile phases: mobile phase A (1% formic acid in water) and mobile phase B (60% mobile phase A and 40% acetonitrile). The elution process was carried out as follows: from minute 0 to minute 10, the proportion of mobile phase B was maintained at 5% of the total mobile phase; from minute 10 to minute 30, the proportion of mobile phase B was increased to 50%, and this proportion was maintained until minute 45; from minute 45 to minute 55, the proportion of mobile phase B was decreased to 5% of the total mobile phase, and this proportion was maintained until minute 60.

The data collected in positive and negative ionization modes using electrospray ionization (ESI) were processed with Compound Discoverer 3.2 (Thermo Scientific™) software. The identification of compounds was facilitated by referencing the mzCloud™ database. A standard solution of 10 ppm concentration was prepared in methanol. Next, 10 μL of the standard solution and 10 μL of the extraction layer were each injected into a UHPLC-ESI-MS/MS system to validate the results against the database. For confirmation purposes, all qualitatively confirmed standards were introduced into a U SCIEX Triple Quad™ 5500 (AB Sciex Pte. Ltd., Estate, Singapore) system coupled with an Exion LC™ AC (AB Sciex Pte. Ltd) system. The concentrations of the standards ranged between 0.01 ppb and 100 ppb. A regression calibration curve was generated to assess the identified compounds [20–22].

2.6. Viability of B16-F10 cells

The B16-F10 melanoma cell line used in this study was purchased from BCRC. To perform the assay, B16-F10 cells were seeded at a density of 1×10^4 cells/well in a 96-well plate and incubated for overnight. Next, the cells were treated with different concentrations of the identified compounds for 24 h. After the incubation, the culture media were removed, and the cells were washed twice with phosphate-buffered saline (PBS). Next, 120 μL of the CCK-8 reagent was added to each well, and the plate was shielded from light and allowed to react in an incubator for 2 h. The absorbance at the wavelength of 450 nm was measured for analysis to determine the effects of different concentrations of the GFE fraction on cell viability [6,20].

2.7. Measurement of melanin content

B16-F10 cells were seeded at a density of 10^5 cells/mL in a 24-well plate and incubated for 24h. After that, the 50 ppm kA (positive control group), 50 ppm of the different GFE fraction were added to cells and were incubated at 37 °C under 5% CO_2 for two days. The cells were washed with 1 mL of PBS twice to remove any residual medium. Next, 200 μL of Trypsin–EDTA was added to each well, and the

plate was incubated for 5 min. Next, each well was rinsed with 800 μL of the culture medium to completely detach the cells. The cell suspensions were then transferred to microcentrifuge tubes and centrifuged at 6000 g for 10 min at 4 °C. The supernatants were discarded. Subsequently, the cells were dispersed in 0.5 mL of 0.1N sodium hydroxide (NaOH) solution and lysed for 60 min at 60 °C to release the melanin content. The resulting solutions were then centrifuged at 12,000 g and 4 °C for 20 min. Next, 100 μL of the supernatant of each solution was collected and analyzed. The absorbance of each sample was measured at 405 nm [6,23,24].

2.8. Melanin concentration in zebrafish

Zebrafish embryos were treated with various compound samples (<100 ppm), KA, or blank at 7–55 h post-fertilization (hpf). At least 35 embryos were used per group and cultured at 28 °C on a 14/10 h light/dark cycle. To measure the melanin concentration, each zebrafish embryo was mixed with 100 μL of Tissue PE LB lysis buffer (supplemented with 100 X protease inhibitor). The mixture was then sonicated using a handheld ultrasonic oscillator, while being kept on ice, for cell disruption. The resulting substance was centrifuged at 13,000 g and 4 °C for 10 min to separate the cellular debris. After centrifugation, the supernatant was removed, and the sediment was mixed with 500 μL of 1 N NaOH solution. The mixture was then placed in a dry bath for 1 h to release the melanin content. Next, 100 μL of the supernatant containing the released melanin content was collected and its absorbance at 405 nm was measured using the plate reader. The measured absorbance values were compared with the standard curve to determine the melanin concentrations in the embryos. After treatment for 48 h (7–55 hpf), the physical appearances of zebrafish embryos were observed using a stereo microscope. The embryos were immobilized with tricaine methane sulfonate and stabilized with 2% carboxymethy1 cellulose sodium salt. Using a tweezer, the position of each embryo was carefully adjusted for lateral and dorsal views to capture photos and videos [6,20].

2.9. Molecular docking simulation

The crystal structure of tyrosinase was obtained from the Research Collaboratory for Structural Bioinformatics Protein Databank (PDB ID: 2Y9X). AutoDockTools was used to remove all water molecules from the receptor and to manually add all hydrogen atoms and Kollman charges [22,25–27]. The structure of each ligand was obtained from the PubChem database. AutoDockTools was employed to remove all water molecules from the receptor and to add all hydrogen atoms and Gasteiger charges. A grid box was created (tyrosinase = 15 Å × 15 Å × 15 Å) along the X-, Y-, and Z-axes, and a grid spacing of 0.375 Å was set to span the protein structure. The grid center of tyrosinase was as follows: X = −10.044, Y = −28.706, and Z = −43.443, and the exhaustiveness value is 8 (the maximum default value) [28–30].

2.10. Statistical analysis

All experiments were conducted at least three times, and the measurement values obtained from each experiment are presented as mean ± standard deviation. All statistical analyses were performed using IBM SPSS 20 (International Business Machines Co., New York, U.S.A.). The differences between the mean values were determined using analysis of variance, and Duncan's multiple range test was used for post hoc comparison. A p-value of <0.05 was considered statistically significant.

3. Results and discussion

3.1. Isolation and purification of the fraction showing tyrosinase inhibitory activity from GFE-EA by Sephadex LH-20 column chromatography

The ethyl acetate fraction of GFE-EA was found to have the most significant inhibitory effect on tyrosinase activity, yielding a half-maximal inhibitory concentration (IC_{50}) value of 118.26 ppm [6]. This study further applied phase partition to purify and collect the subfractions from GFE-EA. To evaluate the anti-melanogenesis effects of the identified compounds, GFE-EA fractions were subjected to *in silico*, *in vitro*, and *in vivo* experiments. A gel filtration chromatography eluted with methanol isolated the GFE-EA fractions. Compared to the control group, certain GFE-EA fractions demonstrated depigmenting effects, as displayed in Fig. S1 (https://doi.org/10.38212/2224-6614.3509). Additionally, it was demonstrated that Sephadex LH-20 column chromatography could be used to rapidly and effectively separate and identify the substances with anti-tyrosinase activity in GFE-EA. Mottaghipisheh et al. (2020) previously demonstrated a successful usage of Sephadex LH-20 column chromatography with organic solvent mobile phases for gel permeation and partition [31]. They successfully purified multiple phenolic compounds, including flavonoid derivatives, and the isolation efficiency was comparable to that achieved in this study. Table 1 shows

the analysis using the Image J software, which indicated that the melanogenesis levels of GFE-EA fractions were lower than the control group, yielding production levels between 79% and 47%. This was comparable to the depigmenting effect of KA in its pure form. The results confirmed that the GFE-EA fractions exhibited substantial inhibitory effects on melanin production. The melanogenesis levels of the groups treated with GFE-EA fractions were lower than the level of the control group. Therefore, the subsequent analysis of the depigmenting compounds was focused on the respective fractions.

3.2. Depigmenting effects of GFE-EA fractions on melanoma cells

In previous fungi-related studies, extracts from *Monascus purpureus*, *Phellinus obliguus*, and *Phellinus vaninii* were examined for anti-melanogenesis effects. Monaspurpyridine from *M. purpureus* at 20 μM significantly reduced melanin production in B16-F10 cells [32]. A polyphenol compound, isolated from *P. obliguus* extracts, showed dose-dependent (from 25 to 200 ppm) decreases in melanin content and tyrosinase activity in melanoma cells [33]. Flavonoids in the methanol extract of *P. vaninii* at 500 ppm reduced melanin content by 39% in B16-F10 cells and inhibited tyrosinase activity by 55.83% at 125 ppm [34]. These findings illustrated the potential of the extracts of natural fungi in reducing melanin synthesis. Specifically, most of the compounds identified as potential anti-melanogenesis agents were aromatic compounds. As displayed in Fig. 1a, 100 ppm of GFE-EA F14 induced a notable cytotoxic effect, yielding cell viability of <80% [35]. Therefore, subsequent test was conducted at concentrations equal to or less than 50 ppm, which was consistent with a previous study on *Ganoderma weberianum*'s impact on cell viability, which conducted on lower extraction concentration at 25 ppm [36]. The results revealed that following a 48-h treatment with 50 ppm GFE-EA F14–F17, the relative melanin concentration in B16-F10 cells significantly decreased from 100% to 82%, as shown in Fig. 1b. Moreover, the melanin content in the cells treated with GFE-EA F17 was similar to that of the positive control group (KA), indicating their comparable inhibitory effects on melanin production. Hsu et al. (2016) previously explored the effects of GFE-EA at 100 ppm on reducing the melanin content in B16-F10 cells. The results confirmed that GFE-EA can inhibit tyrosinase activity, thereby reducing melanin production [6]. In addition, Chen et al. (2021) demonstrated that the hexane partition fraction from *Antrodia cinnamomea* at 100 ppm induced a highly potent tyrosinase inhibitory effect and decreased the pigment content [38]. Compared to a high dielectric constant (DC) solvent, such as water with 80 DC, lower DC solvents like hexane (1.88 DC) and ethyl acetate (6.02 DC) tended to be more efficient in isolating anti-melanogenesis compounds from fungi. This finding was consistent with that of the present study, further validating the depigmenting effects of specific GFE-EA fractions in melanoma cells.

Table 1. Quantification of melanin spots on tyrosinase-based TLC autography.

Relative melanin content	(% of Control)
Con (Negative Control: Methanol)	100%
KA (Positive Control: Kojic acid)	40%
F13	79%
F14	65%
F15	51%
F16	47%
F17	50%

The control group (methanol) was used as the baseline (100% melanin production) to calculate relative melanogenesis rates of the fractions. Kojic acid (KA), a depigmenting compound used in cosmetics, was employed as the positive control group. F13—17: GFE-EA fractions 13–17.

3.3. Depigmenting effects of different GFE-EA fractions in zebrafish embryos

Zebrafish are favored for melanin studies due to their transparent embryos and quick development, allowing facile observation of pigmentation. Moreover, their genetic similarity with humans in melanin synthesis and the feasibility of genetic manipulation make them a cost-effective and ethical alternative to mammalian experimental models [39]. For example, pachymic acid and paeoniflorin in the extracts of Chi-Bai-San, a traditional Chinese herbal medicine, induced 37% and 30.5% decreases in melanin content and tyrosinase activity in zebrafish, respectively, by regulating multiple melanogenic genes [40]. In addition, the ethanol extract of *Hippocampus abdominalis* at 100 ppm significantly reduced melanogenesis in zebrafish larvae by activating the extracellular-signal-regulated kinase signaling pathway [41]. In this study, zebrafish embryo tests were conducted with GFE-EA F13–F17 at concentrations of 25, 50, and 100 ppm. GFE-EA F13 at 100 ppm showed lethal effects, causing complete mortality. GFE-EA F16 at the same concentration led to deformities, similar to *in vitro* results (Fig. 2). Thus, subsequent anti-melanogenesis activity assessments were conducted with 50 ppm of each fraction. The treatment

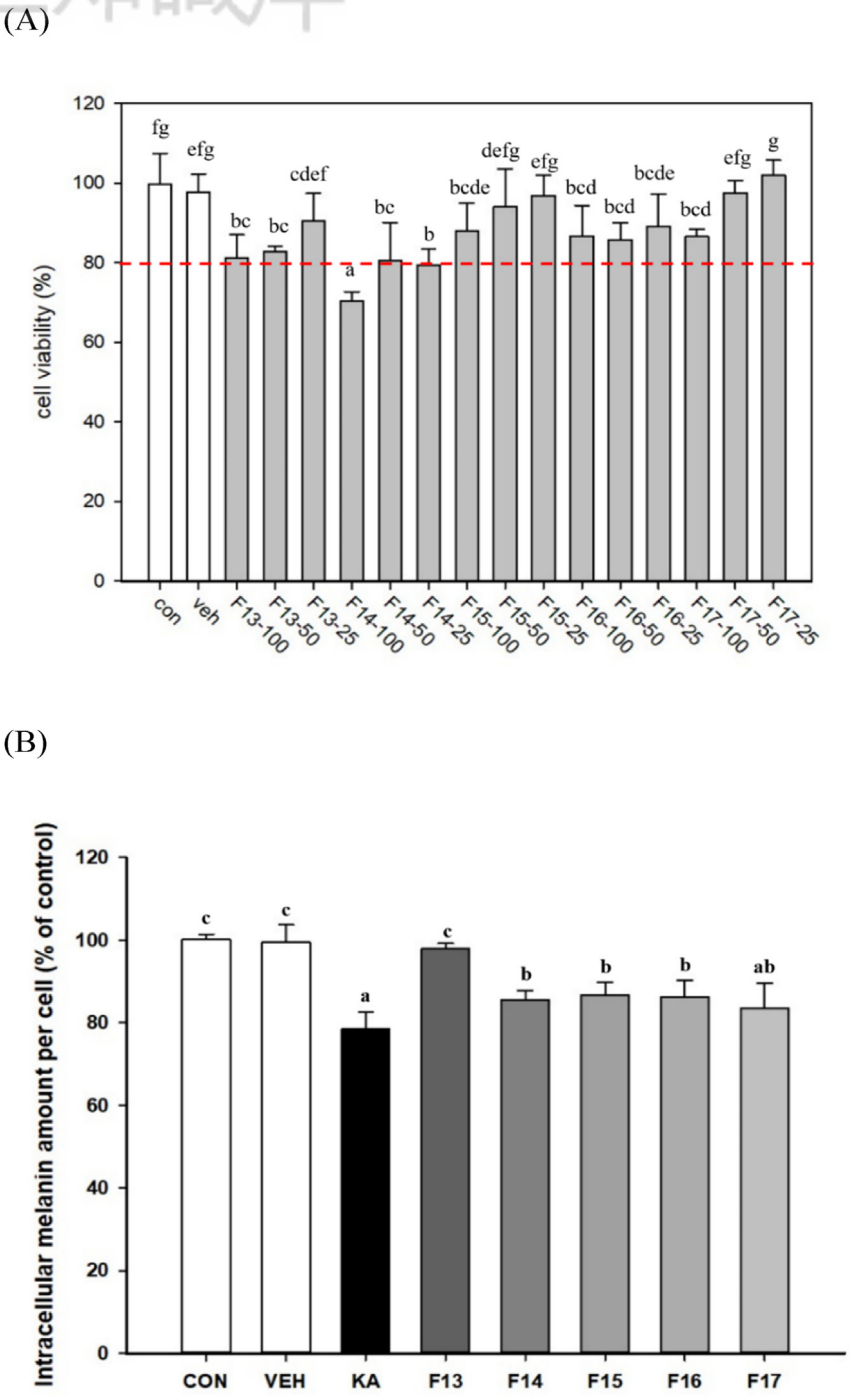

Fig. 1. ***Different concentration of GFE-EA LH-20 F13-F17 treat in B16-F10 melanoma cell.*** *(A) Cell viability; (B) The intracellular melanin content in 50 ppm. *Con: control group. Veh: High-glucose DMEM containing 0.1% DMSO. F13—17: GFE-EA fractions 13—17; KA: Kojic acid.*

with GFE-EA F15, F16, and F17 significantly decreased the relative melanin content to 80%, 83%, and 74%, respectively (Fig. 3). Moreover, the level of melanin content in the GFE-EA F16-treated group was similar to that of the positive control group (KA), indicating that they exhibited comparable depigmenting effects. Hsu et al. (2018) previously used *G. formosanum* mycelium extracts in the concentration range of 50–200 ppm to conduct zebrafish experiments on depigmentation activity [18]. The results confirmed that the extracts contained compounds that could significantly inhibit melanogenesis in zebrafish.

In addition, organic acids and aromatic compounds like isoflavones, pyrones, and terpenes in the ethanol extract of edible mushrooms, at

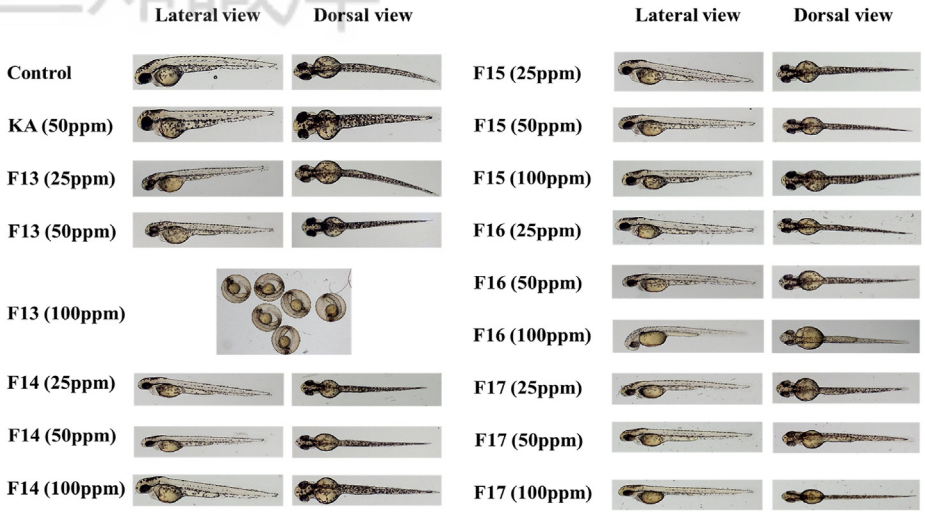

Fig. 2. Depigmenting effect of nontoxic concentration of GFE-EA F13-F17 and kojic acid on melanogenesis of zebrafish in vivo phenotype-based system.

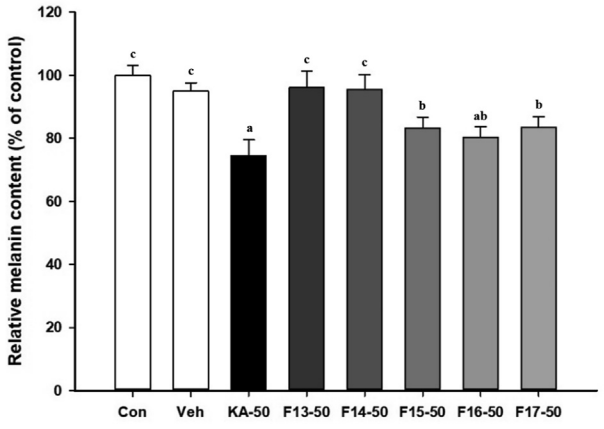

*Fig. 3. **The melanin content of zebrafish after treated with different fractions of GFE-EA LH-20 F13-F17.** Con: control group. Veh: High-glucose DMEM containing 0.1% DMSO. KA: Kojic acid in 50 ppm. F13—17: GFE-EA fractions 13—17 in 50 ppm. In the experiment, the control group comprised untreated zebrafish embryos, and the melanin concentrations were set as 100%. KA was used as a positive control. The aim of the experiment was to measure the amount of melanin produced in a specific number of embryos, thereby determining the melanin concentration per embryo.*

50—100 ppm concentrations, induced depigmenting effects in the melanocytes of zebrafish embryos. The respective activity was attributed to the compounds' alteration of tertiary and quaternary structures of tyrosinase [38,39,42]. This finding provides additional evidence for the depigmenting effects of the compounds extracted from *G. formosanum*, which demonstrated lower working concentrations (50 ppm or lower) in the zebrafish model. Therefore, the subsequent UHPLC-MS/MS analysis focused on the analysis of the compounds present in GFE-EA F15—F17.

3.4. UHPLC-MS/MS of depigmenting compounds derived from GFE-EA F15—17

Fig. S2 (https://doi.org/10.38212/2224-6614.3509) and Table S1 (https://doi.org/10.38212/2224-6614.3509) summarize the results of UHPLC-MS/MS analysis of GFE-EA F15—F17. A total of six compounds, including mesalamine (0.0891 ± 0.0419 ppm), L-pyroglutamic acid (117.8703 ± 48.2877 ppm), esculetin (0.9802 ± 0.3901 ppm), 5-hydroxyindole (0.0447 ± 0.0273 ppm), and salicylic acid (0.0080 ± 0.0073 ppm), were identified in the fractions. These aromatic compounds and organic acids exhibited significant anti-melanogenesis activities.

5-Hydroxyindole is a heterocyclic compound widely known for its anti-tyrosinase properties and its derivatives were identified as potentially having therapeutic value as anti-inflammatory agents [43,44]. Esculetin is a coumarin acid derivative also known for its tyrosinase inhibiting properties, meanwhile recognized to possess immense anti-oxidative potential, thereby alleviating conditions such as arthritis, diabetes, malignancies, and hepatic disorders [45—47]. L-pyroglutamic acid, derived from glutamic acid, is a natural nutrient and an amino acid involved in the glutathione redox cycle that inhibits tyrosinase activity. Guominkang (containing L-pyroglutamic acid), particularly at high concentrations, was found to achieve an effect similar to that of dexamethasone in controlling the symptoms and inhibiting the inflammation of allergic asthma [48,49]. Gluconic acid and its derivatives, including salts and esters, were extensively utilized in the formulation of foods [50]. Gluconic acid possesses hydroxyl and carboxylate

groups and exhibits preservative and chelating characteristics that can inhibit melanin synthesis [51,52]. Salicylic acid, a phenolic compound, acts as a competitive inhibitor of tyrosinase, and can effectively control inflammatory and non-inflammatory acne lesions [53,54]. Mesalamine, a monohydroxybenzoic acid derived from salicylic acid, contains phenol, carboxylic acid, and hydroxybenzoic acid groups, which was recognized to possess immense antioxidative potential, thereby alleviating conditions such as arthritis, diabetes, malignancies, and hepatic disorders [55]. The inhibition of tyrosinase by these compounds was largely due to their hydroxyl groups, with the number and position of the hydroxyls found to critically affect the activity of the enzyme [56]. The inclusion of carboxylic acids and straight-chain fats further enhanced this inhibitory effect [57].

3.5. Single ligand–tyrosinase binding sites explored through molecular docking simulations

Simulations were conducted to ascertain the binding sites and elucidate the mechanisms of tyrosinase (Fig. 4a). The semi-flexible docking approach was applied following previous research, to consider both the calculation amount and the model's predictive ability [58,59]. As shown in

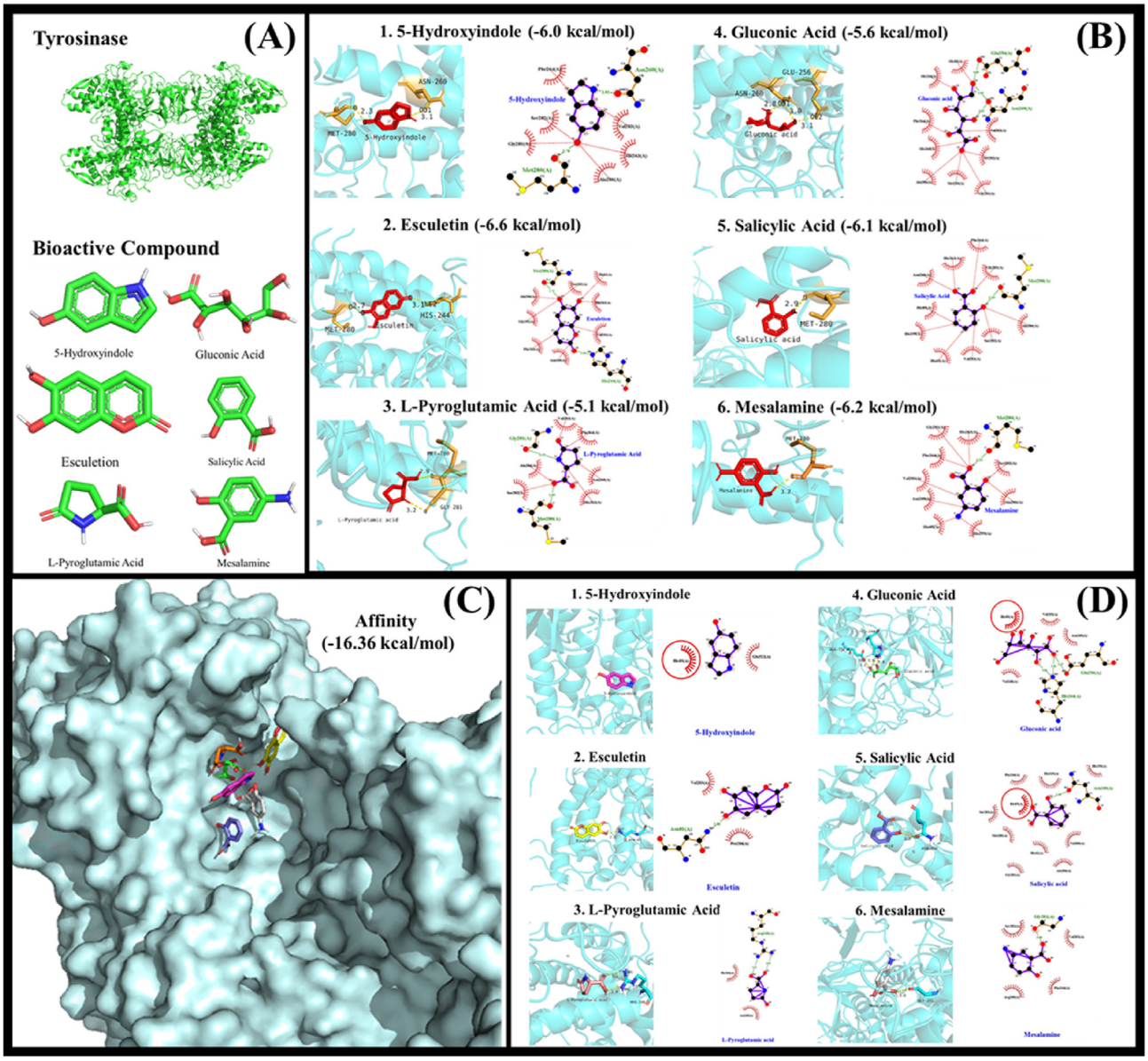

*Fig. 4. **The images and results of molecular docking between anti-melanogenesis compounds and tyrosinase. (A)** Semi-docking protein and ligands; **(B)** Single ligand docking results; **(C)** Multiple ligands docking images; **(D)** Multiple ligands docking results.*

Table 2 and Fig. 4b, single-molecule docking simulations demonstrated that salicylic acid and its derivative, mesalamine, have the highest affinities with affinity scores of −6.1 and −6.2 kcal/mol, respectively. Both compounds were found to form bonds with the Met280 residue of tyrosinase. 5-Hydroxyindole formed hydrogen bonds with the Asn260 and Met280 residues of tyrosinase, showing a binding energy of −6.0 kcal/mol. Esculetin formed hydrogen bonds with the His244 and Met280 residues of tyrosinase, yielding the highest binding energy of −6.6 kcal/mol. Similarly, L-pyroglutamic acid formed hydrogen bonds with the Met280 and Gly281 residues of tyrosinase, showing a binding energy of −5.1 kcal/mol. Gluconic acid formed a hydrogen bond with the Glu256 and ASN260 residues of tyrosinase, showing a binding energy of −5.6 kcal/mol with bond lengths of 3.1, 3.0, and 2.8 Å.

Previous studies have indicated that KA functions as a chelator for Cu2+ ions at the active site of tyrosinase. KA inhibited the tautomerization of dopachrome into 5,6-dihydroxyindole-2-carboxylic acid with an affinity score of −4.09 kcal/mol and interactions with the His85, His259, His263, and Met280 residues. The Met280 residue also bound to the ligands studied in this study, suggesting that the respective ligands may be involved in inhibitory mechanisms similar to those of KA [30,39,45]. The aromatic compounds and organic acids identified in GFE-EA F17 could form hydrogen bonds with tyrosinase inhibitory sites and generate Coulombic forces with multiple residues, thereby effectively inhibiting tyrosinase activity and achieving depigmentation.

3.6. Evaluation of the binding of multiple ligands with tyrosinase through molecular docking simulations

Synergy, where the combined action of multiple components is more effective than the action of a single compound, often leads to better therapeutic outcomes through mutual enhancement and complementation while reducing the side effects [60–62]. Exploring plant-based synergy is complex due to the presence of diverse compounds in phytotherapeutic agents. It is challenging to identify and quantify the effects of individual compounds in the respective agents, especially because they are combined with others [63].

Therefore, multi-molecule docking techniques were adopted and the results were compared with single-molecule docking at the tyrosine kinase inhibitory sites. The differences observed in multi- and single-molecule docking were analyzed to explore the impact of synergy [28].

The simulation calculations yielded an affinity score of −16.36 kcal/mol for the simultaneous interactions between multiple compounds and tyrosinase. When tyrosinase simultaneously interacted with multiple ligands, hydrogen bonds formed with specific amino acid residues, such as Asn81, His244, Glu256, Asn260, Arg268, and Gly281 (Table 2 and Fig. 4d). This docking result was similar to that of epigallocatechin gallate, an ordinary tea-derived polyphenol that acts as a tyrosinase inhibitor, which also forms hydrogen bonds with the Asn81, Cys3, His244, and Asn260 residues of tyrosinase [26,29,30,64,65]. Krobthong et al. (2021) previously performed molecular docking experiments for *Ganoderma* extracts and tyrosinase, and demonstrated that the extracts form hydrogen bonds with the Asn260 and Gly281 residues of tyrosinase. This technique elucidates the inhibition mechanisms of compounds like the VLT peptide against tyrosinase by modeling their binding at the enzyme's active site, estimating their binding affinity, and illustrating crucial interactions, including hydrogen bonds and salt bridges [10].

In recent studies, polar secondary metabolites such as phenolics, flavonoids, and anthocyanins in natural products were focused upon. These compounds were often associated with tyrosinase inhibition due to their capacity to interact with the

Table 2. The concentration of anti-melanogenesis compounds in GFE-EA F17 extraction as well as its binding affinity and interaction with tyrosinase.

Compounds	Concentration (ppm)	Binding Affinity (kcal/mol)		Hydrogen Bonding Interaction	
		Single Ligand	Multiple Ligands	Single Ligand	Multiple Ligands
5-Hydroxyindole	0.0447 ± 0.0273	−6.0	−16.36	Asn-260 Met-280	–
Esculetin	0.9802 ± 0.3901	−6.6		Met-280 His-244	Asn-81
L-Pyroglutamic Acid	117.8703 ± 48.2877	−5.1		Met-280	Arg-268
Gluconic Acid	12.5202 ± 6.7749	−5.6		Asn-260 Glu-256	His-244 Glu-256
Salicylic Acid	0.0080 ± 0.0073	−6.1		Met-280	Asn-260
Mesalamine	0.0891 ± 0.0419	−6.2		Met-280	Gly-281

enzyme and inhibit its function. It was suggested that this inhibition could occur through the chelation of copper ions at the active site or by direct interactions with critical amino acid residues involved in enzymatic activity. Consequently, the enzyme's ability to catalyze the oxidation of phenols to quinones, a crucial step in melanin synthesis, was inhibited [66–68]. However, in this research it was discovered that in addition to aromatic compounds, organic acids in *G. formosanum* extracts also played a potential role as tyrosinase inhibitors. This finding differed from the phenomena previously observed in natural products.

The results indicated that simultaneous interactions of tyrosinase with multiple ligands lead to stronger affinity and molecular binding, resulting in a synergistic effect. Such synergism, in turn, could effectively inhibit the enzyme's activity and lead to more favorable depigmenting outcomes.

4. Conclusion

This study focused on the depigmenting effects of *G. formosanum* and offered significant insights into food nutrition and its practical applications. By employing a variety of chromatography methods, pivotal anti-melanogenesis agents such as gluconic acid, mesalamine, L-pyroglutamic acid, esculetin, 5-hydroxyindole, and salicylic acid were identified in specific GFE-EA fractions. The identified compounds induced a considerable reduction in melanin production in melanoma cells and zebrafish embryos at a considerably low dose of 50 ppm. Moreover, this study adopted molecular docking simulations to investigate the interactions between the identified compounds and tyrosinase. The synergistic interactions of these compounds, highlighted by enhanced binding affinity and a potent inhibition of tyrosinase activity, were more evident when multiple compounds were involved. In summary, this study lays a foundation for future research into food-derived compounds and underscores the pivotal role of edible *G. formosanum* in formulating effective and natural solutions for anti-melanogenesis effects.

Credit author statement

Dr. Chen-Che Hsieh and Dr. Chih-Yao Hou are co-first authors who have the same contribution: Writing Original Draft, Writing, Conceptualization. Darin Khumsupan, Hsiao-Yun Lei, Dr. Pek-Kui Lim, Dr. Cheng-Chih Hsu, and Dr. Kai-Wen Cheng: Data Curation, Formal Analysis. Dr. Sz-Jie Wu: Methodology (Botanical identification). Dr. Kuan-Chen Cheng and Dr. Yi-Chen Chen: Conceptualization; Project Administration and Supervision; proofreading of final manuscript.

Declaration of generative AI and AI-assisted technologies in the writing process

During the preparation of this work the authors used OPENAI in order to polish article. After using this tool, the authors reviewed and edited the content as needed and takes full responsibility for the content of the publication.

Declaration of competing interest

The authors do not declare conflict of interest.

Acknowledgments

This project was funded by the National Science and Technology Council, Taiwan (112-2320-B-002-013-MY3), (112-2221-E-002-040-MY3), and (MOST 108-2926-I-002-001-MY4). The authors would like to thank Dr. Kai-Wen Cheng for providing HPLC MS/MS analyzing and Dr. Yu-Hin Chan for assisting the zebra fish analysis. Also, this article serves as a tribute to Dr. Chan's significant contributions in exploring the anti-melanogenesis properties of *G. formosanum*.

Appendix A. Supplementary data

Supplementary data to this article can be found online.

References

[1] Li Y, Huang J, Lu J, Ding Y, Jiang L, Hu S, et al. The role and mechanism of Asian medicinal plants in treating skin pigmentary disorders. J Ethnopharmacol 2019;245:112173.
[2] Hong YH, Jung EY, Noh DO, Suh HJ. Physiological effects of formulation containing tannase-converted green tea extract on skin care: physical stability, collagenase, elastase, and tyrosinase activities. Integr Med Res 2014;3:25–33.
[3] Chang TT, Chen T. *Ganoderma formosanum* sp. nov. on Formosan sweet gum in Taiwan. Trans Br Mycol Soc 1984;82:731–3.
[4] Hu CM, Cheng HW. Method development for evaluation of hepato-protection functionality of health food. J Food Drug Anal 2000;8:6.
[5] Wang CL, Pi CC, Kuo CW, Zhuang YJ, Khoo KH, Liu WH, et al. Polysaccharides purified from the submerged culture of *Ganoderma formosanum* stimulate macrophage activation and protect mice against *Listeria monocytogenes* infection. Biotechnol Lett 2011;33:2271–8.
[6] Hsu KD, Chen HJ, Wang CS, Lum CC, Wu SP, Lin SP, et al. Extract of *Ganoderma formosanum* mycelium as a highly potent tyrosinase inhibitor. Sci Rep 2016;6:32854.
[7] Chiang CY, Hsu KD, Lin YY, Hsieh CW, Liu JM, Lu TY, et al. The antiproliferation activity of *Ganoderma formosanum* extracts on prostate cancer cells. Mycobiology 2020;48:219–27.

[8] Lai YJ, Hsu KD, Huang TJ, Hsieh CW, Chan YH, Cheng KC. Anti-melanogenic effect from submerged mycelial cultures of *Ganoderma weberianum*. Mycobiology 2019;47:112−9.
[9] Hyde KD, Bahkali AH, Moslem MA. Fungi—an unusual source for cosmetics. Fungal Divers 2010;43:1−9.
[10] Krobthong S, Yingchutrakul Y, Samutrtai P, Choowongkomon K. The C-terminally shortened analogs of a hexapeptide derived from Lingzhi hydrolysate with enhanced tyrosinase-inhibitory activity. Arch Pharm 2021; 354:2100204.
[11] Yu Q, Fan L, Duan Z. Five individual polyphenols as tyrosinase inhibitors: inhibitory activity, synergistic effect, action mechanism, and molecular docking. Food Chem 2019;297: 124910.
[12] Chiang HM, Chen HW, Huang YH, Chan SY, Chen CC, Wu WC, et al. Melanogenesis and natural hypopigmentation agents. Int J Med Biol Front 2012;18:1e76.
[13] Hsu KD, Wu SP, Lin SP, Lum CC, Cheng KC. Enhanced active extracellular polysaccharide production from *Ganoderma formosanum* using computational modeling. J Food Drug Anal 2017;25:804−11.
[14] Ballinger JT, Shugar GJ. Chemical technicians ready reference handbook. McGraw-Hill Education; 2011. ISBN 0071745920.
[15] Lehbili M, Magid AA, Hubert J, Kabouche A, Voutquenne-Nazabadioko L, Renault JH, et al. Two new bis-iridoids isolated from *Scabiosa stellata* and their antibacterial, antioxidant, anti-tyrosinase and cytotoxic activities. Fitoterapia 2018;125:41−8.
[16] Masamoto Y, Ando H, Murata Y, Shimoishi Y, Tada M, Takahata K, et al. Mushroom tyrosinase inhibitory activity of esculetin isolated from seeds of *Euphorbia lathyris* L. Biosci Biotechnol Biochem 2003;67:631−4.
[17] Nakamura M, Ra JH, Jee Y, Kim JS. Impact of different partitioned solvents on chemical composition and bioavailability of *Sasa quelpaertensis Nakai* leaf extract. J Food Drug Anal 2017;25:316−26.
[18] Hsu KD, Chan YH, Chen HJ, Lin SP, Cheng KC. Tyrosinase-based TLC autography for anti-melanogenic drug screening. Sci Rep 2018;8:401.
[19] Es-Safi NE, Cheynier V, Moutounet M. Implication of phenolic reactions in food organoleptic properties. J Food Compos Anal 2003;16:535−53.
[20] Strzępek-Gomółka M, Gaweł-Bęben K, Angelis A, Antosiewicz B, Sakipova Z, Kozhanova K, et al. Identification of mushroom and murine tyrosinase inhibitors from *Achillea biebersteinii Afan. extract*. Mol 2021;26:964.
[21] Hsieh CC, Yu SH, Cheng KW, Liou YW, Hsu CC, Hsieh CW, et al. Production and analysis of metabolites from solid-state fermentation of *Chenopodium formosanum* (Djulis) sprouts in a bioreactor. Food Res Int 2023;168:112707.
[22] Hsieh CC, Yu SH, Kuo HC, Khumsupan D, Huang HC, Liou YW, et al. Glycine-rich peptides from fermented *Chenopodium formosanum* sprout as an antioxidant to modulate the oxidative stress. J Food Drug Anal 2023;31:804−11.
[23] Wang L, Cui YR, Yang HW, Lee HG, Ko JY, Jeon YJ. A mixture of seaweed extracts and glycosaminoglycans from sea squirts inhibits α-MSH-induced melanogenesis in B16F10 melanoma cells. Fish Aquatic Sci 2019; 22:1−8.
[24] Zheng Y, Lee EH, Lee SY, Lee Y, Shin KO, Park K, et al. *Morus alba L.* root decreases melanin synthesis via sphingosine-1-phosphate signaling in B16F10 cells. J Ethnopharmacol 2023; 301:115848.
[25] Hu WJ, Yan L, Park D, Jeong HO, Chung HY, Yang JM, et al. Kinetic, structural and molecular docking studies on the inhibition of tyrosinase induced by arabinose. Int J Biol Macromol 2012;50:694−700.
[26] Hu ZZ, Ma TX, Sha XM, Zhang L, Tu ZC. Improving tyrosinase inhibitory activity of grass carp fish scale gelatin hydrolysate by gastrointestinal digestion: purification, identification and action mechanism. Lebensm Wiss Technol 2022;159:113205.
[27] Hsieh CC, Yu SH, Kuo HC, Cheng KW, Hsu CC, Lin YP, et al. Alleviation of PM2.5-induced alveolar macrophage inflammation using extract of fermented *Chenopodium formosanum* Koidz sprouts via regulation of NF-κB pathway. J Ethnopharmacol 2024;318:116980.
[28] Yu Q, Fan L, Duan Z. Five individual polyphenols as tyrosinase inhibitors: inhibitory activity, synergistic effect, action mechanism, and molecular docking. Food Chem 2019;297: 124910.
[29] Peng Z, Wang G, Zeng QH, Li Y, Wu Y, Liu H, et al. Antioxidant and anti-tyrosinase activity of 1, 2, 4-Triazole hydrazones as antibrowning agents. Food Chem 2021;341: 128265.
[30] Mechqoq H, Hourfane S, ElYaagoubi M, ElHamdaoui A, daSilva Almeida JRG, Rocha JM, et al. Molecular docking, tyrosinase, collagenase, and elastase inhibition activities of argan by products. Cosmetics 2022;9:24.
[31] Mottaghipisheh J, Iriti M. Sephadex® LH-20, Isolation, and purification of flavonoids from plant species: a comprehensive review. Mol 2020;25:4146.
[32] Wu HC, Chen YF, Cheng MJ, Wu MD, Chen YL, Chang HS. Investigations into chemical components from *monascus purpureus* with photoprotective and anti-melanogenic activities. J Fungus 2021;7:619.
[33] Liu YJ, Lyu JL, Kuo YH, Chiu CY, Wen KC, Chiang HM. The anti-melanogenesis effect of 3, 4-Dihydroxybenzalacetone through downregulation of melanosome maturation and transportation in B16F10 and human epidermal melanocytes. Int J Mol Sci 2021;22:2823.
[34] Im KH, Baek SA, Choi J, Lee TS. Antioxidant, anti-melanogenic and anti-wrinkle effects of *Phellinus vaninii*. Mycobiology 2019;47:494−505.
[35] ISO 10993-5, I. S. O. I. Biological evaluation of medical devices—part 5: tests for in vitro cytotoxicity. 2009.
[36] Lai YJ, Hsu KD, Huang TJ, Hsieh CW, Chan YH, Cheng KC. Anti-melanogenic effect from submerged mycelial cultures of *Ganoderma weberianum*. Mycobiology 2019;47:112−9.
[38] Chen HY, Cheng KC, Wang HT, Hsieh CW, Lai YJ. Extracts of *Antrodia cinnamomea* mycelium as a highly potent tyrosinase inhibitor. J Cosmet Dermatol 2021;20:2341−9.
[39] Ferreira AM, de Souza AA, Koga RDCR, Sena IDS, Matos MDJS, Tomazi R, et al. Anti-melanogenic potential of natural and synthetic substances: application in zebrafish model. Mol 2023;28:1053.
[40] Liu SC, Sheu ML, Tsai YC, Lin YC, Chang CW, Lai DW. Attenuation of in vitro and in vivo melanin synthesis using a Chinese herbal medicine through the inhibition of tyrosinase activity. Phytomedicine 2022;95:153876.
[41] Molagoda IMN, Choi YH, Lee S, Sung J, Lee CR, Lee HG, et al. Ethanolic extract of *Hippocampus abdominalis* exerts anti-melanogenic effects in B16F10 melanoma cells and zebrafish larvae by activating the ERK signaling pathway. Cosmetics 2019;7:1.
[42] Pavic A, Ilic-Tomic T, Glamočlija J. Unravelling anti-melanogenic potency of edible mushrooms *laetiporus sulphureus* and *agaricus silvaticus* in vivo using the zebrafish model. J Fungus 2021;7:834.
[43] Karg EM, Luderer S, Pergola C, Buhring U, Rossi A, Northoff H, et al. Structural optimization and biological evaluation of 2-substituted 5-hydroxyindole-3-carboxylates as potent inhibitors of human 5-lipoxygenase. J Med Chem 2009;52:3474−83.
[44] Yamazaki Y, Kawano Y. Inhibitory effect of hydroxyindoles and their analogues on human melanoma tyrosinase. Z Naturforsch C Biosci 2010;65:49−54.
[45] Heleno SA, Barros L, Martins A, Queiroz MJR, Santos-Buelga C, Ferreira IC. Fruiting body, spores and in vitro produced mycelium of *Ganoderma lucidum* from Northeast Portugal: a comparative study of the antioxidant potential of phenolic and polysaccharidic extracts. Food Res Int 2012;46: 135−40.
[46] Zolghadri S, Bahrami A, Hassan Khan MT, Munoz-Munoz J, Garcia-Molina F, Garcia-Canovas F, et al. A comprehensive

review on tyrosinase inhibitors. J Enzym Inhib Med Chem 2019;34:279–309.
[47] Garg SS, Gupta J, Sahu D, Liu CJ. Pharmacological and therapeutic applications of esculetin. Int J Mol Sci 2022;23: 12643.
[48] Chen MY, Wu HT, Chen FF, Wang YT, Chou DL, Wang GH, et al. Characterization of Tibetan kefir grain-fermented milk whey and its suppression of melanin synthesis. J Biosci Bioeng 2022;133:547–54.
[49] Zhou Y, Hu L, Zhang H, Zhang H, Liu J, Zhao X, et al. Guominkang formula alleviate inflammation in eosinophilic asthma by regulating immune balance of Th1/2 and Treg/ Th17 cells. Front Pharmacol 2022;13:978421.
[50] Ramachandran S, Nair S, Larroche C, Pandey A. Gluconic acid. In: Current developments in biotechnology and bioengineering. Elsevier; 2017. p. 577–99.
[51] Eze FN, Nwabor OF. Valorization of Pichia spent medium via one-pot synthesis of biocompatible silver nanoparticles with potent antioxidant, antimicrobial, tyrosinase inhibitory and reusable catalytic activities. Mater Sci Eng C 2020;15:111104.
[52] Zheng Y, Lee EH, Lee SY, Lee Y, Shin KO, Park K, et al. *Morus alba L.* root decreases melanin synthesis via sphingosine-1-phosphate signaling in B16F10 cells. J Ethnopharmacol 2023; 301:115848.
[53] Zhang JP, Chen QX, Song KK, Xie JJ. Inhibitory effects of salicylic acid family compounds on the diphenolase activity of mushroom tyrosinase. Food Chem 2006;95:579–84.
[54] Campos V, Pitassi L, Kalil C, Gonçalves Júnior JE, Sant'Anna B, Correia P. Clinical evaluation of the efficacy of a facial serum containing dioic acid, glycolic acid, salicylic acid, LHA, citric acid, and HEPES in treating post-inflammatory hyperchromia and controlling oily skin in patients with acne vulgaris. J Cosmet Dermatol 2021;20:1766–73.
[55] Gordon GL, Zakko S, Murthy U, Sedghi S, Pruitt R, Barrett AC, et al. Once-daily mesalamine formulation for maintenance of remission in ulcerative colitis: a randomized, placebo-controlled clinical trial. J Clin Gastroenterol 2016;50: 318–25.
[56] Zuo AR, Dong HH, Yu YY, Shu QL, Zheng LX, Yu XY, et al. The antityrosinase and antioxidant activities of flavonoids dominated by the number and location of phenolic hydroxyl groups. Chin Med 2018;13:1–12.
[57] Deering RW, Chen J, Sun J, Ma H, Dubert J, Barja JL, et al. N-acyl dehydrotyrosines, tyrosinase inhibitors from the marine bacterium Thalassotalea sp. PP2-459. J Nat Prod 2016;79: 447–50.
[58] Choi I, Park Y, Ryu IY, Jung HJ, Ullah S, Choi H, et al. In silico and in vitro insights into tyrosinase inhibitors with a 2-thioxooxazoline-4-one template. Comput Struct Biotechnol J 2021;19:37–50.
[59] Song X, Ni M, Zhang Y, Zhang G, Pan J, Gong D. Comparing the inhibitory abilities of epigallocatechin-3-gallate and gallocatechin gallate against tyrosinase and their combined effects with kojic acid. Food Chem 2021;349:129172.
[60] Fujimaki T, Mori S, Horikawa M, Fukui Y. Isolation of proanthocyanidins from red wine, and their inhibitory effects on melanin synthesis in vitro. Food Chem 2018;248: 61–9.
[61] Wagner H, Ulrich-Merzenich G. Synergy research: approaching a new generation of phytopharmaceuticals. Phytomedicine 2009;16:97–110.
[62] Yang Y, Zhang Z, Li S, Ye X, Li X, He K. Synergy effects of herb extracts: pharmacokinetics and pharmacodynamic basis. Fitoterapia 2014;92:133–47.
[63] Williamson EM. Synergy and other interactions in phytomedicines. Phytomedicine 2001;8:401–9.
[64] Wang Y, Zhang G, Yan J, Gong D. Inhibitory effect of morin on tyrosinase: insights from spectroscopic and molecular docking studies. Food Chem 2014;163:226–33.
[65] Marques RV, Guillaumin A, Abdelwahab AB, Salwinski A, Gotfredsen CH, Bourgaud F, et al. Collagenase and tyrosinase inhibitory effect of isolated constituents from the moss *Polytrichum formosum*. Plants 2021;10:1271.
[66] Nakamura M, Ra JH, Jee Y, Kim JS. Impact of different partitioned solvents on chemical composition and bioavailability of *Sasa quelpaertensis Nakai* leaf extract. J Food Drug Anal 2017;25:316–26.
[67] Mostafa IM, Gilani MRHS, Chen Y, Lou B, Li J, Xu G. Lucigenin-pyrogallol chemiluminescence for the multiple detection of pyrogallol, cobalt ion, and tyrosinase. J Food Drug Anal 2021;29:510.
[68] Koyu H, Demir S, Haznedaroglu MZ. Investigation of microwave extraction of red cabbage and its neurotherapeutic potential. J Food Drug Anal 2023;31:4.